Automated Classification of Stellar Spectra. II: Two-Dimensional Classification with Neural Networks and Principal Components Analysis

Coryn A.L. Bailer-Jones[1][*][†], Mike Irwin[2], Ted von Hippel[3]

[1] *Institute of Astronomy, Madingley Road, Cambridge, CB3 0HA, UK*
[2] *Royal Greenwich Observatory, Madingley Road, Cambridge, CB3 0EZ, UK*
[3] *Department of Astronomy, University of Wisconsin, Madison, WI 53706, USA*

ABSTRACT

We investigate the application of neural networks to the automation of MK spectral classification. The data set for this project consists of a set of over 5000 optical (3800–5200 Å) spectra obtained from objective prism plates from the Michigan Spectral Survey. These spectra, along with their two-dimensional MK classifications listed in the Michigan Henry Draper Catalogue, were used to develop supervised neural network classifiers. We show that neural networks can give accurate spectral type classifications ($\sigma_{68} = 0.82$ subtypes, $\sigma_{\rm rms} = 1.09$ subtypes) across the full range of spectral types present in the data set (B2–M7). We show also that the networks yield correct luminosity classes for over 95% of both dwarfs and giants with a high degree of confidence.

Stellar spectra generally contain a large amount of redundant information. We investigate the application of Principal Components Analysis (PCA) to the optimal compression of spectra. We show that PCA can compress the spectra by a factor of over 30 while retaining essentially all of the useful information in the data set. Furthermore, it is shown that this compression optimally removes noise and can be used to identify unusual spectra.

This paper is a continuation of the work done by von Hippel et al. (1994) (Paper I).

Key words: methods: analytical, data analysis, numerical - stars: fundamental parameters

1 INTRODUCTION

The MK classification of stellar spectra (Morgan, Keenan & Kellman 1943; Keenan & McNeil 1976; Morgan, Abt & Tapscott 1978) is an important tool in stellar and galactic astrophysics. In addition to providing fundamental stellar information it was, for example, central to the discovery of nearby Galactic spiral arms (Morgan, Sharpless & Osterbrock 1952; Morgan, Whitford & Code 1953).

MK classification is usually performed by a trained expert visually matching the overall appearance of a spectrum to the 'closest' MK standard spectrum. Such a qualitative method of classification suffers from subjective decisions and may differ from person to person: what is deemed as 'close' by one person may not be 'close' for another. In addition, visual classification is very time consuming, with an expert classifying a few 10^5 stars in a dedicated lifetime. Spectra collected from large spectral surveys, often as a by-product of other surveys (e.g. the Sloan Digital Sky Survey (Kent 1994)) will have to be classified by automated means. Thus if stellar classification is to continue to be useful to the astronomical community, it has to be made faster and put on a more quantitative and objective basis.

In this paper we investigate the application of neural networks to the MK classification of optical stellar spectra. The so-called 'supervised' neural networks used in this project are implemented to yield an accurate mapping between a data domain (the stellar spectra) and a classification domain (the MK classifications). While visual classi-

---

[*] Present Address: Mullard Radio Astronomy Observatory, Cavendish Laboratory, Madingley Road, Cambridge, CB3 0HE, UK
[†] email: calj@mrao.cam.ac.uk

fiers have mentally determined this mapping, they have not quantified it. This mapping is, however, present intrinsically in a large set of classified spectra. The neural network's resultant classification criteria will be essentially equivalent to the human's criteria. However, whereas a human's criteria may vary from adverse physiological and psychological factors such as health and mood, the network will retain a consistent set of classification criteria. We will also demonstrate how the technique of Principal Components Analysis (PCA) can be used to optimally compress the spectra. This has a number of advantages including the preferential removal of noise and an ability to isolate bogus spectra. Furthermore, using PCA-compressed spectra (rather than complete spectra) in the neural network classifiers leads to reduced training times and better convergence stability.

While MK classification will continue to be a useful tool to astronomers, it becomes increasingly desirable to obtain physical parameters (T_{eff}, $\log g$, etc.) for stars. Bailer-Jones et al. (1997b) describe a neural network approach to the parametrization of stellar spectra by training a neural network on synthetic spectra.

2   PREVIOUS CLASSIFICATION WORK

There have been a number of attempts in the past to automate stellar spectral classification. Kurtz (1982) classified low (14 Å) resolution spectra using cross-correlation with standard spectra and achieved a mean classification error of 2.2 spectral subtypes for stars in the range B0 to M2. The same technique gave poor luminosity classification results. LaSala (1994) used the related technique of minimum distance classification to classify a set of 350 B-star spectra, and achieved a mean error of 1.14 spectral subtypes.

The classification work of von Hippel et al. (1994) (Paper I) was one of the first applications of neural networks to stellar spectral classification. Their neural network solution based on a set of 575 spectra gave an RMS classification error of 1.7 spectral subtypes (and a 68-percentile error of 1.4 spectral subtypes) for spectra in the range B3 to M4. Gulati et al. (1994) trained a neural network on a set of 55 spectra giving an incomplete coverage of spectral classes O through to M. While they reported classification errors of 2 subtypes, it should be noted that they used a very complex neural network with over 18,000 free parameters (network weights), with no justification of why such a complex network was required. The result is that the determination of these weights was likely to be poorly constrained by the small amount of training data used.

There have also been attempts to classify spectra beyond the visual. Weaver & Torres-Dodgen (1995) used neural networks to classify infrared spectra (5800 Å to 8900 Å) of A stars at 15 Å, and achieved spectral type and luminosity class classification precisions of 0.4 subtypes and 0.15 luminosity classes respectively. They have recently achieved good results in the infrared for a wide-range of spectral types (O–M) and luminosity classes (I–V) (Weaver & Torres-Dodgen 1997). Vieira & Pons (1995) used a neural network trained on a set of 64 IUE ultraviolet spectra (150 Å to 3200 Å) in the range O3 to G5, and reported a classification error of 1.1 spectral subtypes. It was unclear, however, why a network with 110,000 weights was required.

Table 1. The spectral data.

Plate type	IIaO
Plate size	$\approx 20 \times 20$ cm
	$\approx 5° \times 5°$
	12,000 $\times$ 12,000 pixels
	289 Mb (FITS)
Plate scale	96.62 arcsec mm^{-1}
Dispersion	108 Å/mm at Hγ
Scanning pixel size	15μm
	$\Rightarrow$ 1.45 arcsec pix^{-1}
	$\Rightarrow$ 1.6 Å at Hγ
	(1.05 Å pix^{-1} @ 3802 Å
	2.84 Å pix^{-1} @ 5186 Å)
Coverage of final spectra	3802–5186 Å
Magnitude limit of plates	B $\sim$ 12

Whitney (1983) has examined the use of Principal Components Analysis for spectral classification of a set of 53 A and F stars. His data set consisted of 47 photoelectric measurements of spectra over the wavelength range 3500 Å to 4000 Å. He applied PCA to his data set and then performed a regression on the three most significant components, achieving an average classification error of 1.6 spectral subtypes.

3   THE SPECTRAL DATA

The classification techniques described in this paper were developed using a set of 5000 spectra taken from the Michigan Spectral Survey (Houk 1994). The data reduction method is described in Paper I and in more detail in Bailer-Jones et al. (1997a). The present work expands the data set of Paper I by a factor of ten and doubles the spectral resolution. The wavelength range is also slightly different, with the details summarized in Table 1. The classification information required to train and test the neural networks is taken from the *Michigan Henry Draper* (MHD) catalogue (Houk & Cowley 1975; Houk 1978, 1982; Houk & Smith-Moore 1988). In this paper we only examine the automated classification of normal stars in terms of their MK spectral type and luminosity classes. However, the MHD contains considerable additional information, particularly with regard to peculiarities, so this catalogue would be suitable for developing more detailed automated classifiers.

Our set of 5144 spectra contains stars over a wide range of spectral types (B2–M7) for luminosity classes III, IV and V as well as the 'intermediate' luminosity classes III/IV and IV/V. This set, hereafter referred to as data set 'A', was used to develop a spectral type classifier. A second data set, 'B', contains only 'whole' luminosity classes (i.e. not the III/IV and IV/V spectra). This set of 4795 spectra is used to develop the luminosity class classifier. The distribution of spectral types in this latter set is shown in Figure 1. The spectra were normalized to have equal areas, i.e. equal total intensities, thus removing any scale differences resulting from different apparent magnitudes. Line-only spectra were obtained for both data sets, using a non-linear rectification method (Bailer-Jones et al. 1997a). In this paper we
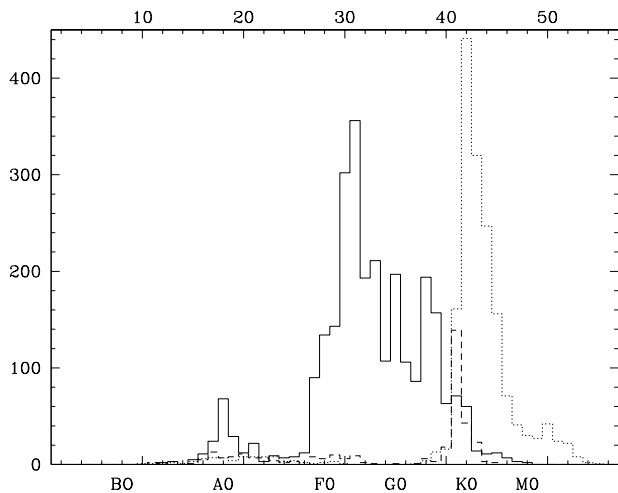
Figure 1. Distribution of spectral types for each luminosity class in data set B. The dotted line represent giants (III), the dashed line subgiants (IV) and the solid line dwarfs (V). The distribution for data set A is very similar.

investigate automated classification with both line-only and line+continuum spectra.

4 NEURAL NETWORK MODELS

A neural network is a computational tool which will provide a general, non-linear parameterized mapping between a set of inputs (such as a stellar spectrum) and one or more outputs (such as a spectral classification). The type of neural network architecture used in this paper is known as a *multilayer perceptron* neural network (e.g. Hertz, Krogh & Palmer 1991; Bishop 1995; Lahav et al. 1996). In order to give the correct input–output mapping, the network is trained on a set of representative input–output data. Training proceeds by optimising the network parameters (the 'weights') to give the minimum classification error. With the weights fixed, the network is used to produce outputs (MK classifications) for unclassified inputs (stellar spectra), effectively by interpolating the training data. Note that the output from a neural network is some non-linear function of *all* of the network inputs. Thus the network's classifications are based on the appearance of the *whole* spectrum: we do not have to tell the network in advance which spectral lines are relevant.

Network training used the methods of gradient descent and backpropagation (Rumelhart, Hinton & Williams 1986). Network performance was found to be insensitive to the exact vaules of the 'gain' and 'momentum' parameters. It was determined that 1000 training iterations were sufficient to ensure that the network error, as evaluated on an independent test data set, had reached its minimum error. Up to 50 times as many iterations gave only negligible improvement. Training a neural network on 2500 spectra represented as 50 PCA coefficients typically took about an hour. The application of these trained networks to then classify a similar number of spectra is a few seconds. Further details can be found in Bailer-Jones (1996).

Spectral type classification was performed by representing the 57 MK classifications in the MHD as points on a

Table 2. Numerical coding of the MK spectral types. 'SpT' will be used to label this code, so that 44 SpT ≡ K2. The MHD catalogue omits some classes (e.g. F4 and G7).

1	O3	18	A0	38	G3
2	O4	19	A1	39	G5
3	O5	20	A2	40	G6
4	O6	21	A3	41	G8
5	O7	22	A4	42	K0
6	O8	23	A5	43	K1
7	O9	24	A6	44	K2
7.5	O9.5	25	A7	45	K3
8	B0	26	A8	46	K4
8.5	B0.5	27	A9	47	K5
9	B1	28	F0	48	M0
10	B2	29	F2	49	M1
11	B3	30	F3	50	M2
12	B4	31	F5	51	M3
13	B5	32	F6	52	M4
14	B6	33	F7	53	M5
15	B7	34	F8	54	M6
16	B8	35	G0	55	M7
17	B9	36	G1	56	M8
17.5	B9.5	37	G2	57	M9

continuous scale of numbers 1–57 (Table 2). This is reasonable as we know that spectral type is closely related to effective temperature (T_{eff}) and MK spectral types are essentially binnings of a continuous sequence. The appropriate neural network therefore had a single output giving a continuous number in the range 1–57. We shall refer to this as *continuous mode*. Note that although the network is trained on integer or half-integer values, it can produce any real-value classification for new spectra.

For the luminosity class problem, we used a network in *probabilistic mode*. This refers to a network with several outputs, each output referring to a mutually exclusive class. In our case we had three outputs, with one output corresponding to each of classes III, IV and V. In this mode, the values in each node can be interpreted as the probability that the input spectrum is of that particular luminosity classes. Probabilistic interpretation of neural networks in both probabilistic mode (also referred to in the neural network literature as 'classification') and continuous mode (also referred to as 'regression') can be taken much further. In particular, the outputs can be interpreted as Bayesian posterior probabilities (e.g. Richard & Lippmann 1991; MacKay 1995).

4.1 Committee of Networks

Identical neural networks trained from different initial random weights should ideally converge on the same weights and hence produce identical input–output mappings. However, given the high dimensionality and complexity of the error surface which is explored during training, it is unlikely that numerical minimization procedures with different initializations would converge on exactly the same final weight vector.

We can reduce the effects of this 'convergence noise' problem by using a *committee of neural networks*. The committee consists of L identical networks which are separately

trained from different initial weights. When the network is used in continuous mode, the committee classification of the pth spectrum, $\overline{C^p}$, is just the average of the individual network classifications. In probabilisitic mode, the outputs from each network corresponding to a given class are summed to give the (unnormalized) committee probability of that class. In some applications, $\overline{C^p}$ will be a more accurate classification than any of the individual network classifications (Bishop 1995). All classification results presented in this paper were obtained with a committee of ten neural networks.

4.2 Neural Network Error Measures

The performance of a trained neural network (or committee thereof) is evaluated by comparing its classifications of an independent set of spectra with their 'true' classifications in the MHD catalogue. We must not evaluate the performance of the neural network using the data on which it was trained. This is because it is possible for the network to overfit the training data rather than capture the underlying input–output mapping which the training data represent. This can occur if there is either insufficient data to constrain the determination of the network weights, or if the training data is not representative of the problem in hand. Such an overfitted network would typically produce very low classification errors on the training data yet produce relatively large errors on an independent test data set. Our procedure was therefore to train a network on half of the spectra and test its performance on the other half, there being approximately 2500 spectra in each half.

We use the following error measures to evaluate the performance of our networks. The first is the RMS error, $\sigma_{\rm rms}$, of the difference between the network classifications and the 'true' classifications. This statistic suffers from the usual problem that it is sensitive to outliers and may not, therefore, be very characteristic of the majority of residuals in the core of the distribution. A more robust measure uses only the central 68% of the residuals, σ_{68}. If the residuals are distributed as a Gaussian, σ_{68} is the 1σ standard deviation of a Gaussian distribution. Both $\sigma_{\rm rms}$ and σ_{68} are *external* errors, because they are measured with respect to a set of ideal classifications which are external to the neural network.

Due to the 'convergence noise' problem (section 4.1), a network re-trained from different initial weights would give slightly different classifications. This level of difference is characterised by the *internal* error and is evaluated using the committee of networks. The internal error for a single spectrum is:

$$\sigma_{int}^p = \sqrt{\frac{1}{L-1}\sum_{l=1}^{l=L}(C_l^p - \overline{C^p})^2} \quad . \tag{1}$$

C_l^p is the classification given by the lth network in the committee. The total internal error, $\sigma_{\rm int}$, is σ_{int}^p averaged over all spectra, and can be considered as the contribution to the total (external) error on account of imperfect network convergence.

An additional consequence of the 'convergence noise' is that a single value of the external error, σ_{68}, is not exact. Thus if we wish to compare values of σ_{68} produced by different network models, then we need to know the uncertainty
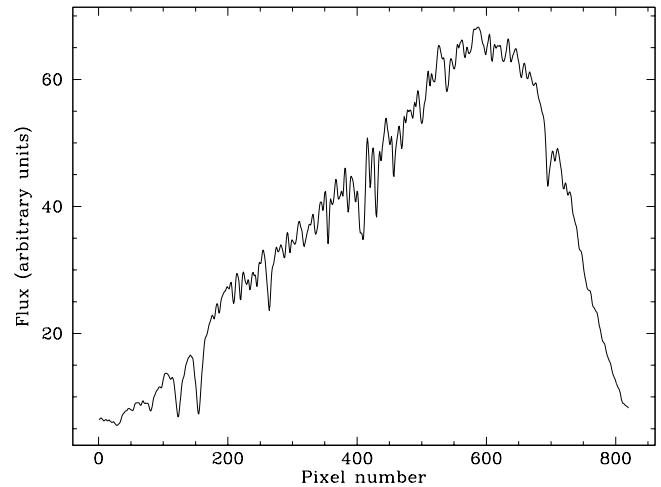
Figure 2. Average spectrum for line+continuum version of spectra in data set A.

in σ_{68} in order to known whether the difference between two values of σ_{68} is statistically significant. A suitable measure of this uncertainty is given by the standard error in the σ of a Gaussian distribution,

$$\varepsilon = \frac{\sigma_{68}}{\sqrt{2M}} \quad , \tag{2}$$

where M is the number of spectra in the test set. This result holds exactly in the limit as $M \to \infty$.

5 PRINCIPAL COMPONENTS ANALYSIS

It is usually desirable – and often essential – to reduce the dimensionality of a data set prior to classification. Dimensionality reduction often leads to enhanced reliability when using neural networks to give a generalized mapping, on account of the reduced number of parameters in the network. This will also lead to greatly reduced training times. While classification with complete spectra can produce good results (Paper I), dimensionality reduction may be essential in some applications, such as when data transmission rates from space-based observatories are limited (e.g. Lindegren & Perryman 1996).

Principal Components Analysis (PCA) is one method for achieving a dimensionality reduction. PCA is a method of representing a set of N-dimensional data by means of their projections onto a set of r optimally defined axes. As these axes (the *principal components*) form an orthogonal set, PCA yields a *linear* transformation of the data. A compression of the data is obtained by ignoring those components which represent the least variance in the data. The compressed spectra, as represented by their projections, onto the most significant principal components, are then used as the neural network inputs. In this section we will demonstrate the benefits of a PCA preprocessing of spectra, such as noise removal and identification of bogus spectra, and highlight some of its problems. In the next section we shall demonstrate that high quality classifications can be achieved with these compressed spectra.

Below we discuss the application of PCA to the line+continuum spectra of data set A. A separate analysis

was carried out for the line-only spectra (Bailer-Jones 1996). PCA has been used in several areas of astronomy, including stellar spectral classification (Deeming 1964; Whitney 1983; Storrie-Lombardi et al. 1994), galaxy spectral classification (Folkes, Lahav & Maddox 1996) and quasar spectral classification (Francis et al. 1992). Further details of the technique can be found in texts (e.g. Murtagh & Heck 1987).

5.1 The Principal Components

PCA was performed on zero-mean spectra: the subtracted average spectrum, $\overline{\mathbf{x}}$, is shown in Figure 2. Figure 3 shows the first ten principal components, $\mathbf{u}$, plotted on a common vertical scale. Because the principal components are eigenvectors of a symmetric matrix, they are orthogonal, and it is convenient also to normalize them to unit length, so that $\mathbf{u}_i^T . \mathbf{u}_j = \delta_{i,j}$. As the eigenvectors are simply rotations in the N-dimensional data space of the original axes on which the spectra are defined, they resemble spectra, in particular in that they have the same number of elements (820) as the original spectra.

It is interesting that both the stellar continuum and the individual spectral lines are distributed across many eigenvectors. For example, the Ca II H&K lines at 3934 Å and 3969 Å are distinct in the first four eigenvectors as well as the average spectrum. (Note that the sign of the eigenvectors is arbitrary, as the admixture coefficients – the projections of the spectra onto the principal components – can be negative.) That the features do not separate into different components is not surprising: We known from the physics of line formation in stellar photospheres that a spectrum is not a linear combination of spectral features, so we should not expect a linear decomposition of the spectrum (such as PCA) to clearly isolate these spectral features. Features are generally distributed across many components, e.g. components 5 and 8 which show many lines common to a wide range of spectral types. However, some features are predominantly represented by a single components. For example, it can be seen that the TiO bands (which extend redward from about 4500 Å) characteristic of M stars are more strongly represented in the 7th principal component than any other component.

The principal components represent sources of variance in the data. Thus the most significant principal components show those features which vary the most between the spectra: it is important to realise that the principal components do not simply represent strong features. Note also that the eigenvectors obtained from PCA are entirely dependent on the data. Therefore the eigenvectors for a different set of stellar spectra are likely to be rather different.

5.2 The Admixture Coefficients

The projection of the pth spectrum onto the kth principal components is known as the *admixture coefficient*, $a_{k,p}$. Because PCA is only a linear transformation of the spectra, one would not expect there to be a strong correlation between the stellar classification parameters and the admixture coefficients. Figure 4 shows the admixture coefficients for the line+continuum spectra plotted against the coded MK spectral type, SpT, for each of the first ten eigenvectors shown

in Figure 3. No single coefficient shows a strong correlation across the full range of subtypes, so classification cannot be achieved using any one coefficient. Some coefficients do, however, show correlations over part of the spectral range. We saw in Figure 3 that the 7th eigenvector represents some features of late-type stars and we see in Figure 4 that the corresponding admixture coefficient, shows a trend with spectral type for SpT $\gtrsim 48$.

5.3 PCA as Data Compression and Noise Filter

The most significant principal components contain those features which are most strongly correlated in many of the spectra. It follows that noise – which is uncorrelated with any other features by definition – will be represented in the less significant components. Thus by retaining only the more significant components to represent the spectra we achieve a data compression that preferentially removes noise. The *reduced reconstruction*, $\mathbf{y}_p$, of the pth spectrum $\mathbf{x}_p$, is obtained by using only the first r principal components to reconstruct the spectrum, i.e.

$$\mathbf{y}_p = \overline{\mathbf{x}} + \sum_{k=1}^{k=r} a_{k,p}\mathbf{u}_k \quad , \qquad r < N \ . \tag{3}$$

Let $\boldsymbol{\varepsilon}_p$ be the error incurred in using this reduced reconstruction. By definition, $\mathbf{x}_p = \mathbf{y}_p + \boldsymbol{\varepsilon}_p$, so

$$\boldsymbol{\varepsilon}_p = \sum_{k=r+1}^{k=N} a_{k,p}\mathbf{u}_k \quad . \tag{4}$$

Averaging over all spectra gives rise to the average error, $\mathcal{E}$, from which we define the figure-of-merit of the reconstruction quality of the whole data set as $R = 1 - \mathcal{E}$, and

$$R = 100\% \frac{\sum_{k=1}^{k=r} \lambda_k}{\sum_{k=1}^{k=N} \lambda_k} \quad , \tag{5}$$

where λ_k is the kth eigenvalue of the covariance matrix, $\mathbf{S}$, of the data (Bailer-Jones 1996). Figure 5a shows how R varies with the number of eigenvectors used to reconstruct the spectra, and Table 3 tabulates some of these values. We see that only 25 eigenvectors ($\sim 3\%$ of the total) are sufficient to reconstruct 95.8% of the variance in the data. This large factor of data compression is a great benefit for any approach to the classification problem as it corresponds to a large reduction of the dimensionality of the space required to describe the data.

It is convenient to define an empirical measure of the reconstruction error for individual spectra

$$E = \frac{100\%}{S} \sum_{i=1}^{i=N} |y_{i,p} - x_{i,p}| \quad , \tag{6}$$

where S is the total area under each spectrum, which was fixed to a constant value when the spectra were area normalized. This measure is useful as it does not require the existence of eigenvalues for its evaluation, and hence can be used to compare reconstruction errors between any data compression techniques. The frequency distribution of these errors is shown in Figure 6.

Figure 7 gives a visual presentation of spectral reconstruction by showing an M star spectrum reconstructed with
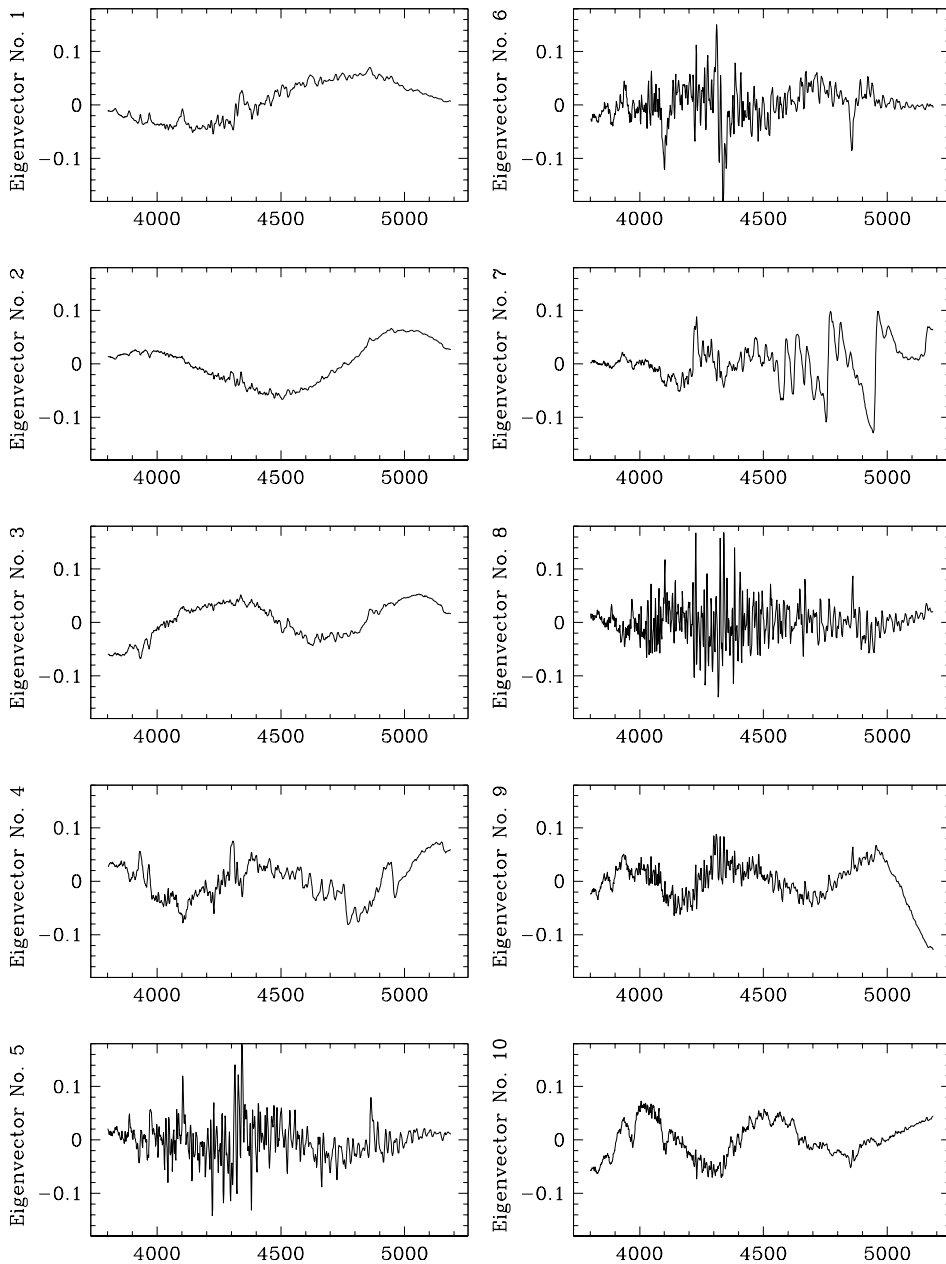
Figure 3. The first ten principal components of the line+continuum spectra in data set A. The principal components are normalized eigenvectors plotted against wavelength. A number of spectral features can be seen. In particular, the 7th eigenvector strongly represents the TiO bands of late-type stars.

an increasing number of components. We have seen in Figure 3 that the 7th eigenvector is representative of the TiO bands in late type stars. In reconstructing this M star spectrum we see that the reconstruction error drops significantly when the 7th component is added, and that visually this $r = 7$ spectrum is greatly improved over the $r = 6$ one.

An optimal trade-off between compression (and noise removal) and accurate spectral representation is achieved for $r = n$ when $\frac{dR}{dn} \approx const$. If a PCA were performed on a data set of pure noise, no component would be a greater discriminant than another, and their ranking would be random giving $\frac{dR}{dn} = const$ for all n. Turning this argument around, the point where the R-n plot levels off ($\frac{dR}{dn} \approx const$) is where

the components begin to be dominated by noise. This occurs between $n = 20$ and $n = 30$ (Figure 5b). Figure 8 compares a faint spectrum reconstructed with 25 components with the original spectrum. The reconstructed spectrum is considerably less noisy and the residual spectrum contains no major features. Note that if we had lower S/N data, $\frac{dR}{dn}$ would turn constant at a smaller value of N. Thus for lower S/N data, the optimality criterion translates into retaining fewer components.

One of the drawbacks of PCA is that very weak spectral features or features which are only present in a small fraction of the data will be lost in a reduced reconstruction. This is because they show very little correlation across the data
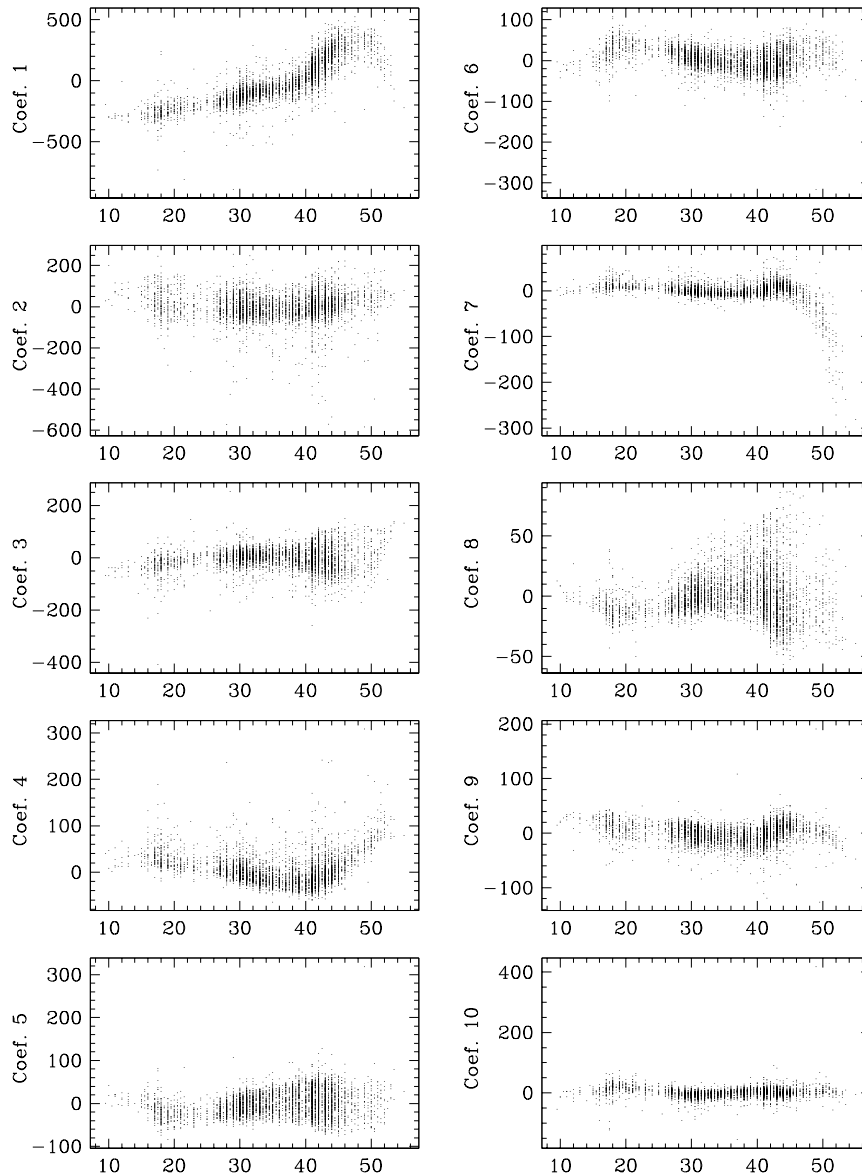
Figure 4. The first ten principal component admixture coefficients for all spectra (line+continuum format) in data set A plotted against spectral subtype (SpT). The correlation between the 7th coefficient and spectral subtype for SpT $\gtrsim 48$ (M stars) is accountable by reference to Figure 3 where we see that the 7th eigenvector gives a strong representation of the TiO features in M stars. In general, however, the admixture coefficients cannot be used individually to give spectral type classifications.

set. Thus the residual spectrum will contain, in addition to noise, some weak features which are not well correlated across the spectra. However, as can be seen from Figure 8, by no means are all such features are lost. Thus we see that the principal components (like neural network classifiers) are sensitive to the relative frequency of occurrence of features in the data set. An advantage of this is that PCA can be used to filter out bogus features (e.g. plate scratches, strong cosmic rays) because such features are rare and randomly positioned. This is demonstrated in Figure 9.

5.4   Constructing New Spectra

Having performed PCA on a set of stellar spectra (the *construction set*), we may want to find the admixture coefficients for a new set of data, such as more recently acquired spectra. We do not have to re-evaluate the principal components using the combined data sets: instead we can project the new spectra onto the old components. We can even obtain the admixture coefficients for incomplete spectra, thus permitting a complete reconstruction. This would be useful if we wanted to apply the neural network classifier to new spectra with a slightly different wavelength coverage.
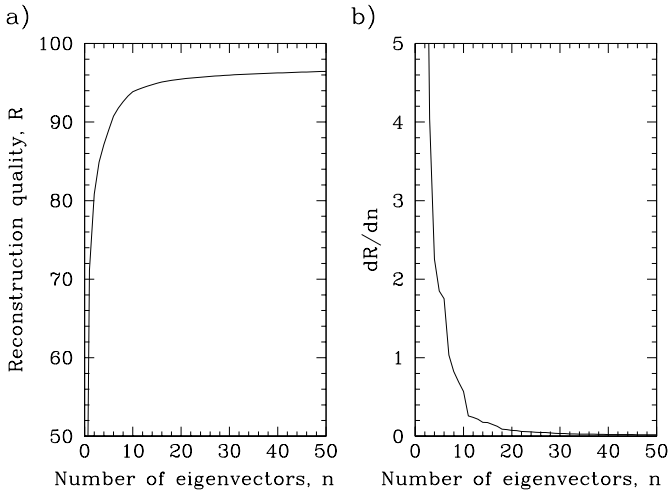
a)

b)

Figure 5. Quality of spectral reconstruction with a reduced number of eigenvectors. a) The quality of reconstruction increases dramatically over the first 25 or so eigenvectors. b) At $n \approx 25$, $\frac{dR}{dn} \approx 0$, and the remaining eigenvectors are predominantly noise. Thus an optimal reconstruction only requires approximately the first 25 eigenvectors. R is the reconstruction error predicted by the eigenvalues (equation 5) and so is the reconstruction error for the whole data set.

Table 3. Selected values from Figure 5.

Number of Eigenvectors	$R(= 1 - E)$	dR/dn	d^2R/dn^2
1	71.135	–	–
2	80.840	9.705	−61.430
3	84.884	4.044	−5.661
4	87.139	2.255	−1.789
5	88.989	1.850	−0.405
10	93.861	0.570	−0.119
15	94.930	0.174	−0.004
20	95.458	0.074	−0.012
25	95.760	0.052	−0.005
30	95.972	0.036	−0.002
35	96.121	0.027	−0.001
40	96.244	0.023	−0.001
45	96.352	0.021	−0.000
50	96.449	0.018	−0.001
820	100.000	0.000	0.000

Another advantage of PCA is that the reconstruction error, E, can be used to filter-out bogus and non-stellar spectra, as in such cases the reconstruction error would be larger than the typical values in Figure 6. As an example, Figure 10 shows how this filtering works by attempting to reconstruct sky noise. The 25-component reconstruction gives an error of 28%, which is several times larger than the maximum reconstruction error of the spectra in the construction set.

This method of rejection assumes that the data used to define the principal components are representative of the stellar spectra which we want to classify. Thus rare types of stars with strong features, e.g. Me stars, would be filtered out along with all the bogus spectra. Note that a neural network applied to either the complete spectra or the PCA
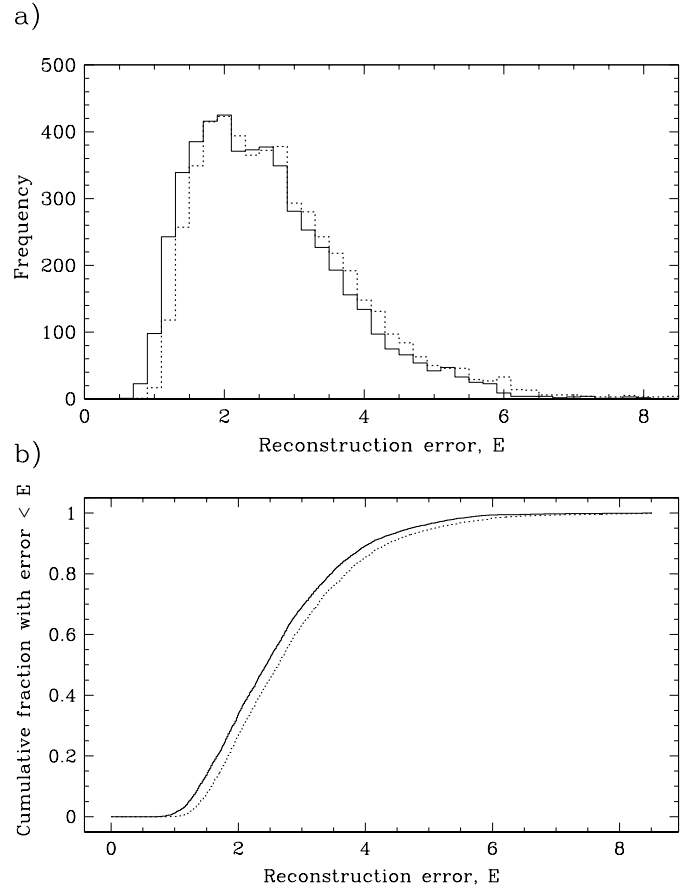
a)

b)

Figure 6. Frequency distribution of the empirical reconstruction error defined by equation 6. The solid line shows the errors for a 50-component reconstruction and the dashed line for a 25-component reconstruction. (a) histogram of the reconstruction errors. (b) the cumulative distribution of (a). This shows the fraction of spectra which are reconstructed with an error less than that shown on the horizontal axis. For example, 95% of the spectra have $E < 4.6\%$.

compressed spectra suffers from a similar problem: spectral types which are relatively rare in the training data set will be poorly classified. But with PCA there is no reason why such objects have to be blindly rejected: A large reconstruction error indicates an unknown object, so PCA could be used as a coarse front-end classifier to a more refined classification system.

6 SPECTRAL TYPE RESULTS

Neural networks were applied to the spectral type problem in continuous mode (see section 4). Each spectrum is represented by the admixture coefficients of the first 25 or 50 principal components. Data set A is used throughout.

Figure 11 shows classification results using a committee of ten networks applied to the 50-component line+continuum PCA spectra. Each network has a 50:5:1 architecture, indicating 50 nodes in the input layer, 5 nodes in the hidden layer and a single output (numbers exclude bias nodes). The average classification error is $\sigma_{68} = 1.07$ SpT, which has an associated uncertainty of $\varepsilon = 0.02$ SpT,
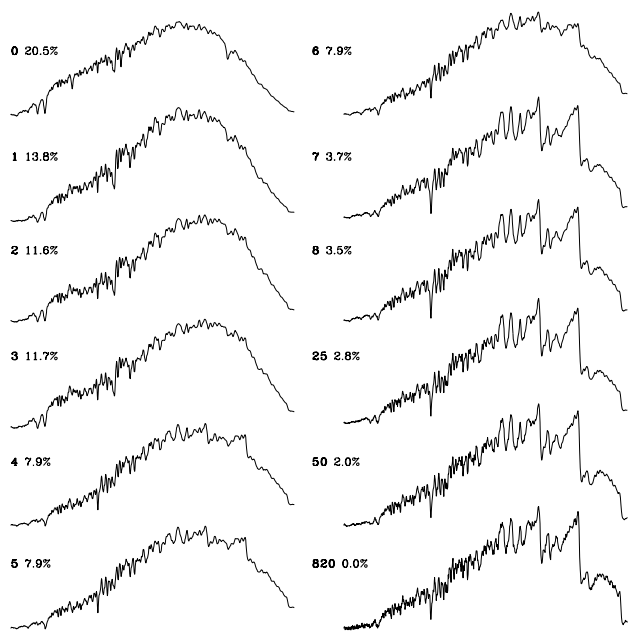
Figure 7. Reconstruction of an M star (HD 14002, type M3/4 III, magnitude 9.4). The figures in bold refer to the number of eigenvectors used to reconstruct the spectrum. The percentage figures are the corresponding reconstruction error, E. Note the improved reconstruction as the 7th component is added.
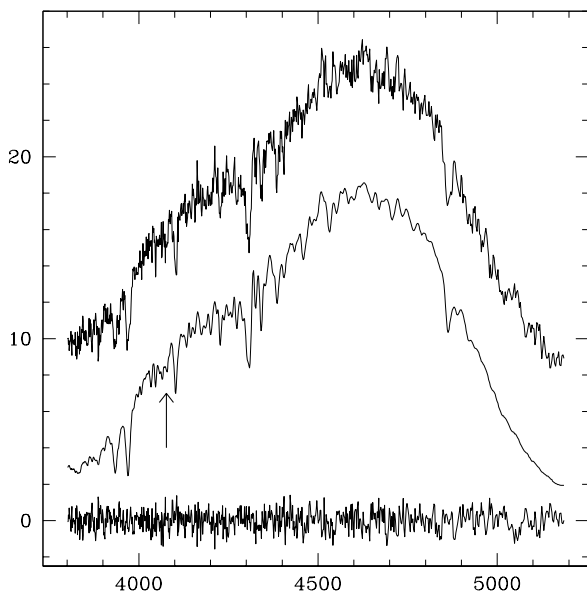

Figure 8. Reconstruction of a faint G star (HD 219795, G3 V, magnitude 11.1). The reconstruction error is $E = 4.26\%$. The top spectrum is the original spectrum, the middle is the spectrum reconstructed with 25 components and the bottom is the residual spectrum, i.e. reconstructed minus original. The arrow marks the location of a weak luminosity sensitive line Sr II which is retained in the reconstruction. This spectrum is one of the faintest (and hence noisiest) in the data set, so most reconstructions are considerably better.
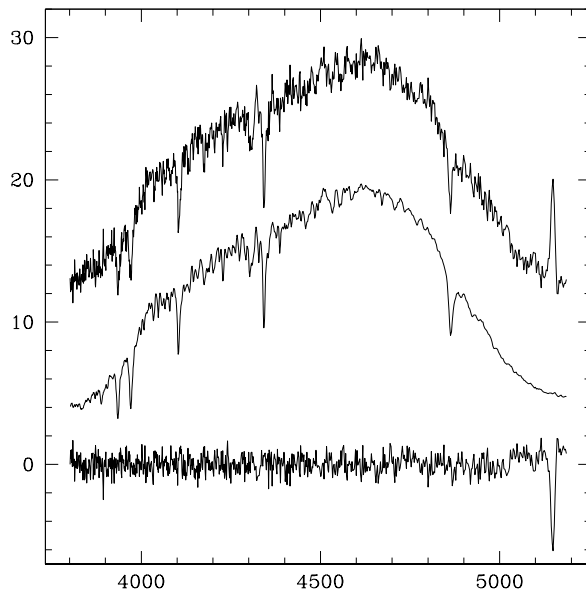

Figure 9. The use of PCA in filtering out bogus features. (See caption to Figure 8.) The contaminating feature here is probably due to a piece of dust on the plate during plate scanning. The star is HD 3391, type F5 V, magnitude 10.8. The reconstruction error is $E = 5.30\%$.

i.e. $\sigma_{68} = 1.07 \pm 0.02$ SpT. $\sigma_{\rm rms} = 1.41$ SpT, indicating that the tails of the distribution of the residuals are 'heavier' than we would get if the distribution were Gaussian.

The optimality criterion for reconstructing spectra (section 5.3) specified that 25 principal components would give an optimal reconstrutcion. However, this figure was achieved without any reference to how we would subsequently use the spectra. A direct evaluation of the number of principal components required is shown in Figure 12, which summarizes the performance of networks with an r:5:1 architecture for a range of r. The behaviour is well anti-correlated with the behaviour of the reconstruction quality, R, in Figure 5. This is what we would expect and demonstrates that the network is making best use of the information given to it.

As the number of hidden nodes in the network increases, so does its ability to accurately model increasingly complex input–output functions. Figure 13 shows how the classification errors vary with the number of hidden nodes These results show that as q is increased to about seven, there is an improvement in classification performance, but beyond this there is no statistically significant improvement. (Note that the neural network with only one hidden node can only linearly discriminate between spectral types, which explains the sharp decrease in classification error between $q = 1$ and $q = 2$.) A network with $q = 250$, gave $\sigma_{68} = 1.00 \pm 0.01$ SpT, which is a small increase over $q \approx 5$. While it is theoretically true that a sufficiently large number of hidden nodes will increase performance (Hornick, Stinchcombe & White 1990), the number of hidden nodes required would be inhibitively large, both on account of training time and over-fitting the data. The solution is to use an additional hidden layer. This can provide increased complexity with a smaller total number of weights. A committee of ten 50:5:5:1 neural networks gave a classification error of $\sigma_{68} = 0.88 \pm 0.01$ SpT, which

Table 4. Summary of the spectral type classification results using committees of ten networks for a variety of architectures. The error measures in columns 3–6 are defined in section 4.2.

Network Architecture	Spectral Format	σ_{68} (SpT)	ε (SpT)	$\sigma_{\rm rms}$ (SpT)	$\sigma_{\rm int}$ (SpT)	No. of Weights
25:3:1	line+continuum	1.11	±0.015	1.43	0.19	82
25:5:1	line+continuum	1.11	±0.015	1.46	0.18	136
50:5:1	line+continuum	1.07	±0.015	1.41	0.24	261
25:5:5:1	line+continuum	0.86	±0.012	1.16	0.33	166
50:5:5:1	line+continuum	0.88	±0.012	1.16	0.47	291
820:5:5:1	line+continuum	0.82	±0.011	1.18	0.15	4141
25:3:1	line-only	1.09	±0.015	1.43	0.28	82
25:5:1	line-only	1.04	±0.015	1.37	0.34	136
50:5:1	line-only	1.03	±0.014	1.35	0.41	261
25:5:5:1	line-only	0.82	±0.011	1.09	0.36	166
50:5:5:1	line-only	0.86	±0.012	1.15	0.56	291
25:25:25:1	line-only	0.86	±0.012	1.15	0.53	1326
MHD class. (Houk)	photographic plates	0.63	–	–	0.44	?
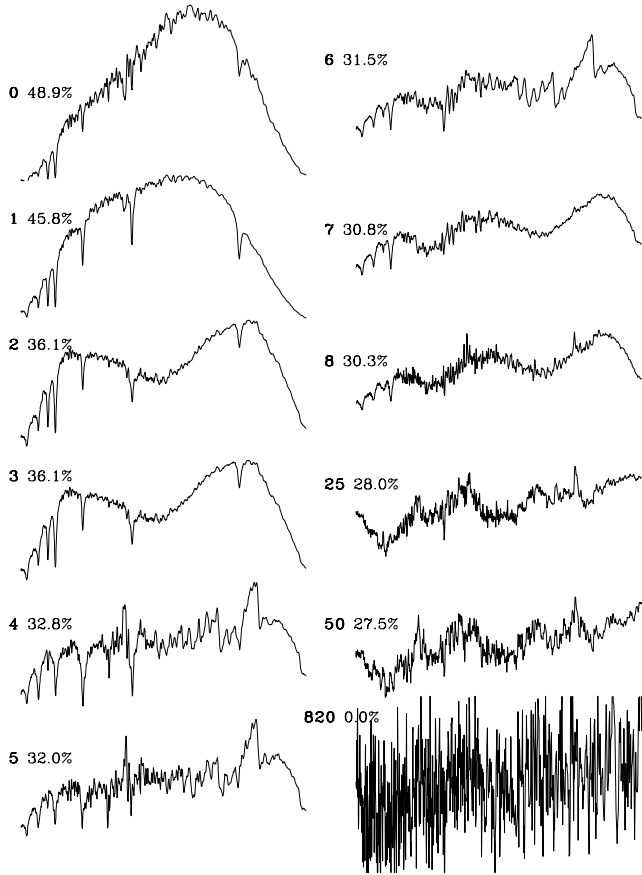
Figure 10. Bogus spectra (in this case a patch of sky) are reconstructed with a large error, which can be used to filter them out of the data set prior to classification. The figures in bold refer to the number of eigenvectors used to reconstruct the spectrum. The percentage figures are the corresponding reconstruction error, E.

is significantly better than the results with only one hidden layer.

Table 4 is a summary of the spectral type classification results obtained with a range of network architectures.
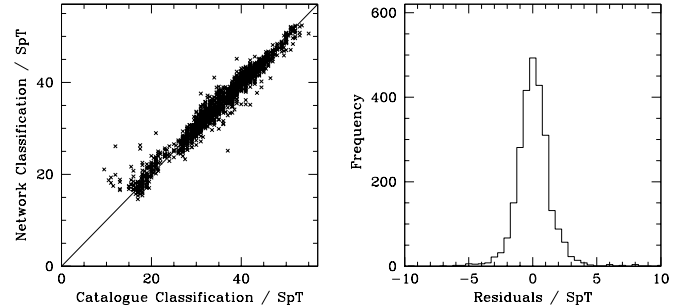
Figure 11. Spectral type classification results from a committee of ten 50:5:1 neural networks applied to line+continuum spectra. The left-hand panel is a plot of the committee classifications against the 'true' classifications listed in the MHD catalogue. The diagonal line is the locus of points for which the committee classifications equal the catalogue classifications, and is drawn to guide the eye. Note that even a perfect classifier would not give results exactly on this line on account of noise in the spectra and uncertainty in the 'true' classifications. The right-hand panel is a histogram of the classification residuals, $\overline{C^p} - G^p$, where $\overline{C^p}$ is the committee classification and G^p the catalogue classification of the pth spectrum. The classification error is $\sigma_{68} = 1.07$ SpT.

The most significant result is that smaller external errors (σ_{68} and $\sigma_{\rm rms}$) are obtained with two hidden layers compared with one hidden layer. Interestingly, the internal error is smaller when the total number of weights is smaller, presumably because the minimum of the error function is easier to locate consistently when the dimensionality of the space is lower. This is one reason for using PCA to compress the spectra, as it results in a network with fewer weights.

Our results also show a very small improvememnt in classification performance when using line-only spectra. This is perhaps to be expected as the continuum is more contaminated by effects such as interstellar reddening and non-linear photographic response. It is interesting that von Hippel et al. (1994) (Paper I) obtained worse results with line-only spectra. This is probably because they used spectra at half the resolution, resulting in the loss of some line-information (whereas the continuum would hardly be affected).
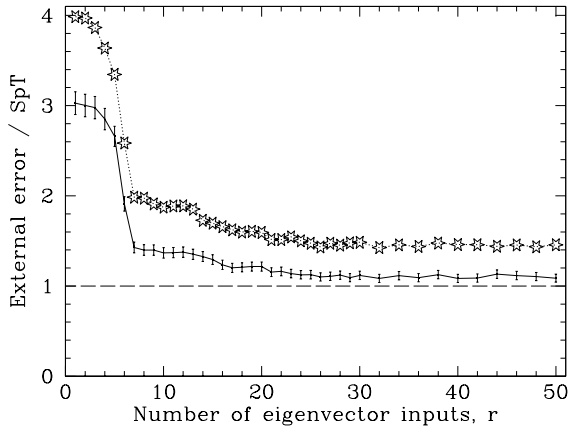
Figure 12. Variation of network classification (external) error, as a function of number of PCA inputs to the neural network. The solid line is σ_{68} and the dotted line is σ_{rms}. The number of inputs, r, is the number of principal components used to represent each spectrum. The error bars on the lower curve are $3 \times \varepsilon$ errors (see equation 2). Statistically speaking, there is a significant drop in the classification error from $r = 1$ to $r \approx 25$, followed by a barely significant decrease in error to $r = 50$.
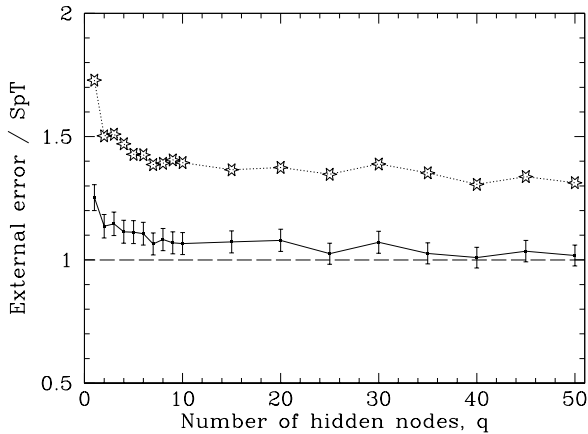

Figure 13. Variation of the network classification (external) error as a function of the number of hidden nodes, q, in a 50:q:1 neural network. For each value of q a single neural network was trained using line+continuum spectra and its performance assessed by measuring σ_{68} (solid line) and σ_{rms} (dashed line). The error bars are $3 \times \varepsilon$, where ε is the statistical uncertainty in σ_{68}.

The best results are plotted in Figure 14. Table 5 lists the σ_{68} error achieved by each neural network in this committee and confirms empirically that the error obtained by the ten networks acting as a committee is lower than any one of the networks acting alone. Figure 15 shows graphically the degree of reproducibility of results. The committee result of $\sigma_{68} = 0.82$ compares quite favourably with the error in the catalogue classifications themselves, estimated to be $\sigma_{68} = 0.63$ SpT (N. Houk, private communication, 1995), which represents a lower limit on the precision we can achieve. Larger networks did not improve performance further.

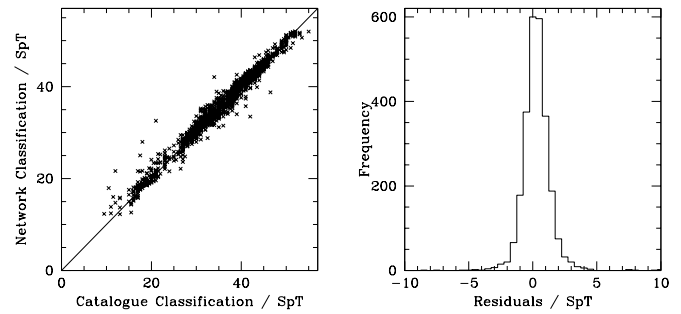To prove that the PCA was not limiting the performance of the neural network classifiers, we trained a com-

Figure 14. Best spectral type results ($\sigma_{68} = 0.82$ SpT), obtained with a committee of ten 25:5:5:1 networks with line-only spectra.

Table 5. Spectral type classification errors for each member a committee (25:5:5:1 networks on line-only spectra). The committee error is lower than the error achieved by any one of its members acting alone. The dispersion of results for individual network is typical of the other committees used in the spectral type problem.

Network	σ_{68}	σ_{rms}
1	0.90	1.21
2	0.86	1.23
3	0.87	1.09
4	0.89	1.27
5	0.93	1.24
6	0.91	1.21
7	0.87	1.17
8	0.95	1.31
9	0.89	1.13
10	0.87	1.17
Committee	**0.82**	**1.09**
σ_{int}	**0.36**	

mittee of neural networks on the original (non-PCA) 820-bin spectra. The mean classification error of $\sigma_{68} = 0.82$ SpT shown in Table 4 is no better than the PCA-input results for comparable numbers of hidden nodes, confirming that the PCA compression has not resulted in the loss of any classification-significant information. Strictly speaking, this 820:5:5:1 network has too many weights to be well-determined by the data (4141 weights (unknowns) vs. 2500 spectra (equations)), so it may be surprising that such a network can generalize. However, due to correlations between the spectral features, some input weights will be correlated, effectively reducing the number of parameters which must be determined by the data. Indeed, the Principal Components Analysis showed that the effective dimensionality of the spectra is only about 25.

The internal and external error measures we have been using are averages over all spectral types. Figure 16 shows that σ_{68} and σ_{int} vary considerably as a function of spectral type. This is influenced by the frequency distribution of spectral types: As we can see from comparison with Figure 1, where there are relatively few spectra in the training set the classification errors are correspondingly higher. This is because the neural network has been presented with relatively
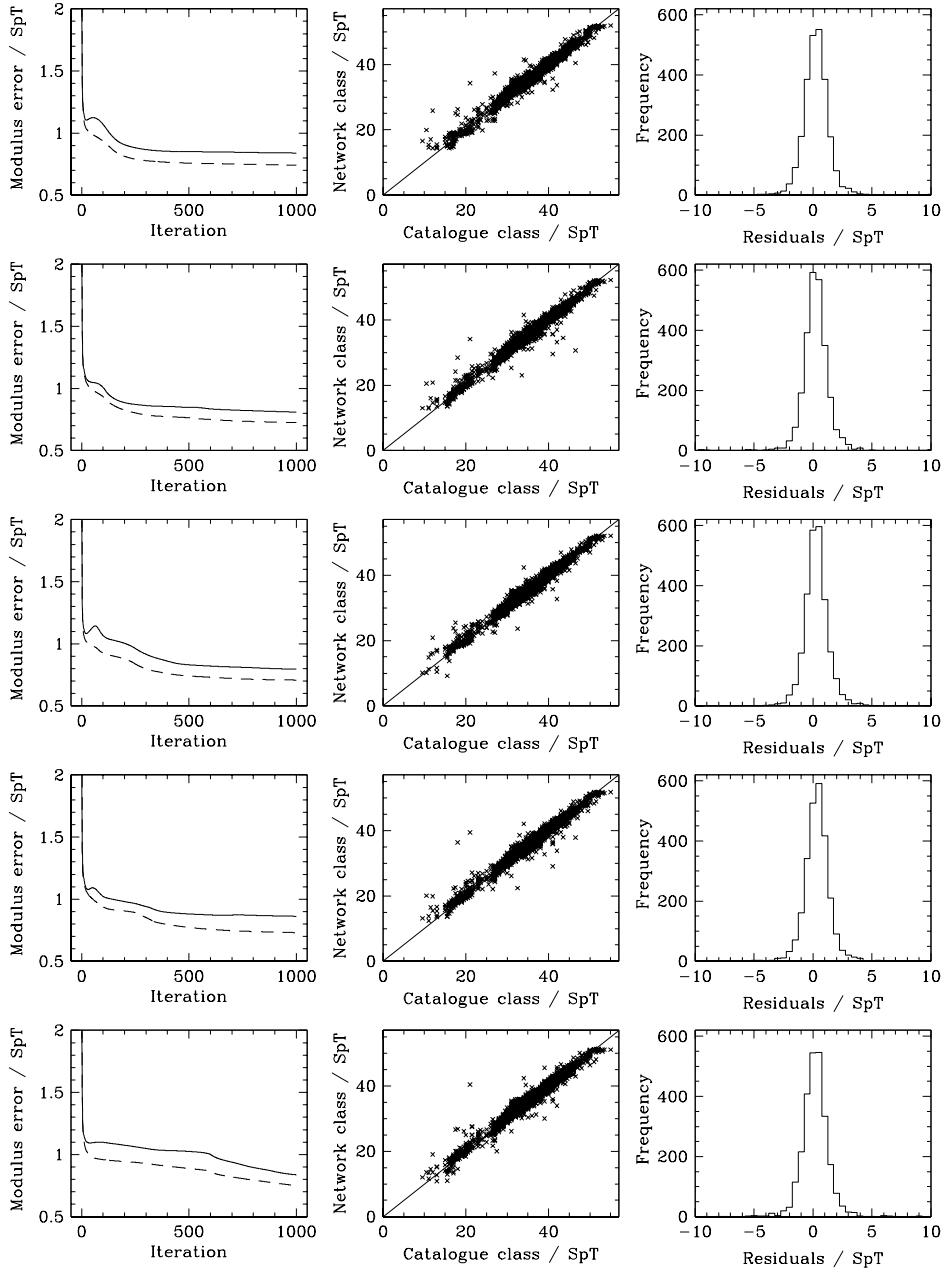
Figure 15. Performance of the first five members of the committee networks used to produce the results in Figure 14. The left-hand figures show how the neural network error drops with increasing iteration number. The dashed line shows the error on the training set and the solid line the error on the test set. Note that the network error, as measured on the test set during training, briefly *increases* early on in the training for the first and third networks. This demonstrates that we should not stop training the instant that the error on the test set rises. It is also interesting that most of the training takes place in the first few iterations.

little information about these regions, and the few spectra are unlikely to give adequate information on the intra-class variability. Indeed, if we remove the few spectra at the earliest and latest spectral types, our overall error drops towards the limit imposed by the training data.

We have also experimented using neural networks in probabilistic mode for spectral type classification. A committee of ten such 50:5:5:57 networks applied to the line+continuum spectra gave $\sigma_{\mathrm{rms}} = 2.09$ SpT, which is somewhat inferior to continuous output results. However,

the probabilistic approach does offer some advantages, such as the ability to recognise composite spectra (Weaver 1994).

7   LUMINOSITY CLASS RESULTS

Neural networks were applied to the luminosity class problem in probabilistic mode (see section 4) using data set B. The spectrum is classified as that class for which the output is highest. We only consider two-hidden layer networks.

The measure of network performance when we have a

Table 6. Confusion matrices for four different committees of ten networks. Each confusion matrix lists the percentage of spectra which have been classified correctly and incorrectly. Thus from the top-left matrix we see that the committee correctly classifies 97.7% of class Vs as class Vs, but incorrectly classifies 1.5% of spectra which are class V in the catalogue as class III. The rows of each matrix sum to 100%.

25:5:5:3, line+cont. spectra

Network Class

		III	IV	V
Catalogue Class	III	92.0%	2.1%	5.9%
	IV	43.8%	11.4%	44.9%
	V	1.5%	0.8%	97.7%

25:5:5:3, line-only spectra

Network Class

		III	IV	V
Catalogue Class	III	91.4%	2.7%	5.9%
	IV	42.7%	14.1%	43.2%
	V	1.6%	1.2%	97.2%

50:5:5:3, line+cont. spectra

Network Class

		III	IV	V
Catalogue Class	III	92.6%	1.7%	5.8%
	IV	44.3%	9.7%	46.0%
	V	1.3%	0.6%	98.1%

50:5:5:3, line-only spectra

Network Class

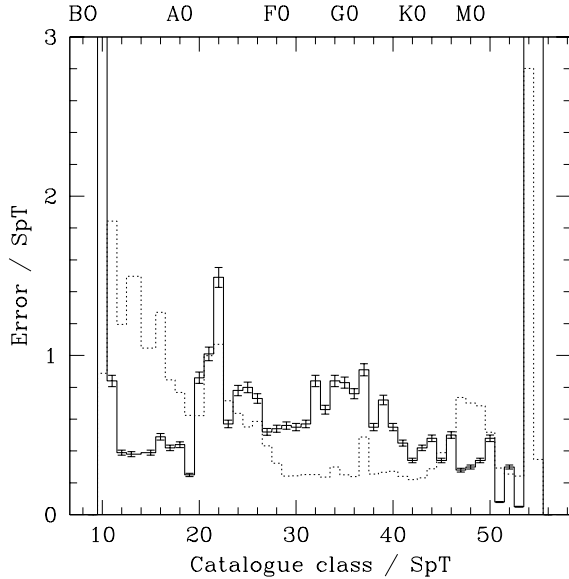|		III	IV	V
Catalogue Class	III	90.9%	3.4%	5.7%
	IV	42.2%	14.1%	43.8%
	V	2.0%	1.6%	96.4%

Figure 16. Neural network classification errors as a function of spectral type. The solid line is the external error, σ_{68}, and the dotted line the internal error, σ_{int}. The error bars on the external error histogram are $3 \times \varepsilon$ errors for each spectral type bin, showing that the differences are significant. These results are from the committee of ten 25:5:5:1 neural networks applied to line+continuum spectra shown in Table 4.

few discrete classes is by means of the *confusion matrix*. This reports the fraction of spectra which have been correctly and incorrectly classified for each class. Table 6 compares the results from different committees of networks, with the four combinations of line-only or line+continuum spectra represented with 25 or 50 principal components. We see that

there is little difference in performance between any of these combinations. This is in agreement with the spectral type classifications and confirms that most of the luminosity class information is contained within the first 25 admixture coefficients. The networks give very good results for classes III and V (but not class IV), although the better results for class V than class III may be due to larger fraction of class Vs in the data set (1.6 times as many).

Figure 17 shows the distribution of the probabilities which the committee assigns for each class. While most of the class III and V objects are correctly classified with large confidence, the opposite is true for class IVs. The network is not classifying IVs at random (otherwise we would expect it to classify about 33% correct). Rather, the networks have a preference for classifying IVs as either IIIs or Vs. While the relative paucity of class IVs in the training set will have some influence, they are not so rare to give such poor performance. Nor are the IVs lower quality spectra.

Referring back to Figure 1 we see that there is a fairly strong correlation between spectral type and luminosity class. Is the network using spectral type information to produce luminosity classifications? It would do quite well if it simply classified all spectra later than about K0 as giants and the rest as dwarfs. (Note that much of this correlation is real, because the HR diagram is not uniformly populated.)

To find out what spectral information the networks are using, an 'overlap' data set was created by selecting spectra of classes III, IV and V in roughly equal numbers for that range of spectral types where their frequency distributions overlap (around G6). These spectra were then classified using a committee previously trained on all the data. We see from Table 7 that the committee still yields good classifications of classes III and V, for which it cannot be using spectral type information as there is no correlation between spectral type and luminosity class over this specif-
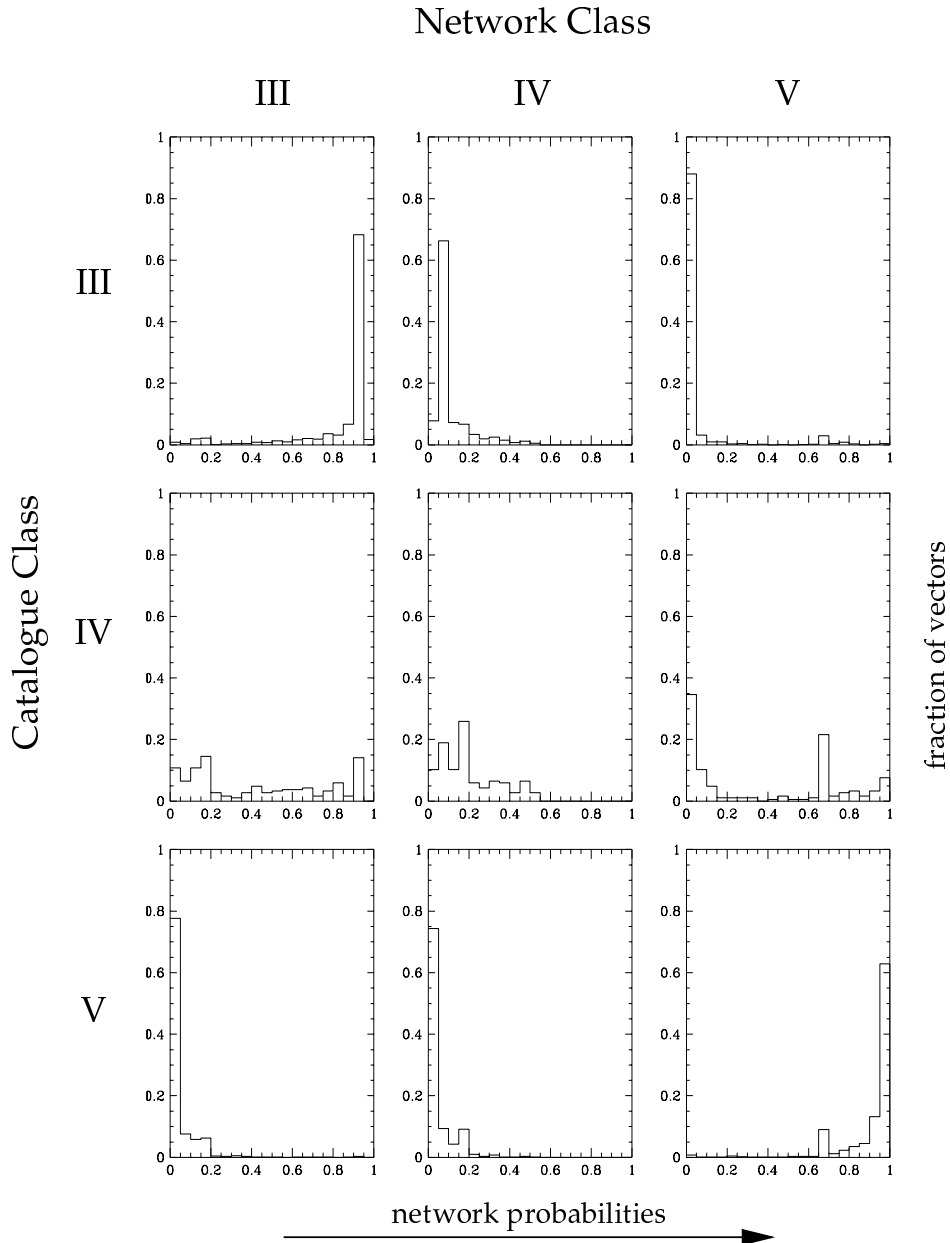
Network Class

Figure 17. Distribution of class probabilities assigned by the three outputs of a committee of ten 50:5:5:3 networks trained on line+continuum spectra. Each plot is a histogram of the committee probabilities for a certain network class (column) and a certain catalogue class (row). For example, the bottom-left hand diagram shows the distribution of the committee probabilities from the class III output node for spectra which are catalogue class V, and shows that most catalogue class V objects have been assigned a low probability of being class III. Each plot in a given row includes the same spectra, and this number has been used to normalize the fractions for that row. The total numbers of IIIs, IVs and Vs in the test data set are 848 IIIs, 185 IVs and 1364 Vs, with almost exactly the same numbers in the training set. Due to the nature of the sigmoid function in the neural network we can never achieve 100% confidence.

ically chosen and narrow spectral range. There must, therefore, be independent luminosity information present in this 50-component reconstruction of the stellar spectra. The class IV classifications are still poor.

The failure on class IV spectra implies that, at the resolution of these spectra, class IV stars are not spectroscopically distinct from either class III or class V. Certainly, visual classifiers find it hard to distinguish class IVs from IIIs and Vs around late G-type stars (N. Houk, private commu-

nication, 1996). It cannot be due to the PCA compression as complete spectrum classification gives almost exactly the same results as shown in Figure 6. Problems with the data reduction, e.g. imperfectly registering the spectra in wavelength, could also contribute. An alternative explanation is as follows. Visual classifiers can focuse on certain lines in a spectrum and disregard all others. In principal, neural networks can do this too by altering their weights. However, when there is noise in the spectrum some inputs will show

Table 7. An 'overlap' data set is classified using the committee of ten 50:5:5:3 networks trained on line+continuum spectra. This overlap data set consists of those spectral classes for which the three luminosity classes are equally represented, which is for spectral types G5/G6, G6, G6/G8 and G8. This data set consists of 86 IIIs, 83 IVs and 68 Vs. The committee still classifies IIIs and Vs well and still fails on IVs (cf. Table 6).

50:5:5:3, line+cont. spectra, G6-G8 spectra only

Network Class

		III	IV	V
	III	87.2%	8.1%	4.7%
Catalogue Class	IV	56.6%	20.5%	22.9%
	V	4.4%	2.9%	92.7%

random correlations with the target outputs. Thus the network will make a small level of false inference about the relevance of certain inputs in determining the outputs. With class IV discrimination the relevance of the few truly important features may have been washed out this false 'noise association'. A solution to this problem is to use prior knowledge of which lines are relevant and train the network only on those features. Another approach is *automatic relevance determination* (MacKay 1995), which is a Bayesian technique for assessing the relevance of the inputs using the evidence in the data.

We attempted to use networks with two continuous outputs to tackle the spectral type and luminosity class problems simulataneously. However, the results were inferior, with the best results being $\sigma_{68} = 1.53$ SpT ($\sigma_{\rm rms} = 2.02$ SpT) for the spectral type and $\sigma_{68} = 0.15$ ($\sigma_{\rm rms} = 0.4$) luminosity classes (Bailer-Jones 1996). Due to the spectral type–luminosity class correlation in the data set, the network may be unable to adequately separate out luminosity effects from temperature ones. This is not helped by the weakness of the luminosity distiguishing features in this wavelength region. In order to tackle both problems simultaneously, we may need a more complex model, and such complexity may not be available with modest-sized networks.

8 SUMMARY

We have produced a system for the automated two-parameter classification of stellar spectra over a wide range of spectral types (B2–M7) based on a large (> 5000), homogenous set of spectra. We have shown that we can achieve classification errors of $\sigma_{68} = 0.82$ subtypes ($\sigma_{\rm rms} = 1.09$ subtypes) over this complete range of spectral subtypes. This result compares favourably with the intrinsic errors of $\sigma_{68} = 0.63$ subtypes in our training data. Once a neural network has been trained, its classification results are completely reproducible. Moreover, the low values of their internal errors (< 0.4 spectral subtypes) demonstrate that networks can be re-trained to give sufficiently consistent classifications.

We have achieved correct luminosity class classification for over 95% of dwarfs (class V) and giants (class III). Results for luminosity class IV spectra were considerably worse. It is believed that the data themselves could be a limiting factor and methods for improving these results were discussed. Despite the correlation in the data set between spectral type and luminosity class, it was demonstrated that the neural networks were using luminosity features to do dwarf-giant discrimination.

Network with two hidden layers performed considerably better (≈ 0.2 subtypes) than ones with only one hidden layer. The best classification results were achieved by tackling the spectral type and luminosity class problems separately, using continuous and probabilistic networks respectively.

We used Principal Components Analysis to compress the spectra by a factor of over 30 while retaining 96% of the variance in the data. It was shown that this compression predominantly removes noise. In addition the PCA preprocessing reduces the dimensionality of the data and can be used to filter out bogus spectral features or identify unusual spectra. However, PCA has the drawback that very weak or rare features will not be well-reconstructed. More complex non-linear preprocessing schemes could no doubt be devised, but the strength of PCA is its analytic simplicity and its robustness.

The automated classifiers presented in this paper have been used to produce classifications for several thousand stars which do not have classifications listed in the MHD catallogue. These will be presented in a future paper (Bailer-Jones 1998).

REFERENCES

Bailer-Jones C.A.L., 1996, PhD thesis, Univ. Cambridge
Bailer-Jones C.A.L., 1998, in preparation
Bailer-Jones C.A.L., Irwin M., von Hippel T., 1997a, MNRAS, submitted
Bailer-Jones C.A.L., Irwin M., Gilmore G., von Hippel T., 1997b, MNRAS, 292, 157
Bishop C.M., 1995, Neural Networks for Pattern Recognition. Oxford Univ. Press, Oxford
Deeming T.J., 1964, MNRAS, 127, 493
Folkes S.R., Lahav O., Maddox S.J., 1996, MNRAS, 283, 651
Francis P.J., Hewett P.C., Foltz C.B., Chaffee F.H., 1992, ApJ, 398, 476
Gulati R.K., Gupta R., Gothoskar P., Khobragade S., 1994, ApJ, 426, 340
Hertz J., Krogh A., Palmer R.G., 1991, Introduction to the Theory of Neural Computation. Addison-Wesley, Redwood City
Hornick K., Stinchcombe M., White H., 1990, Neural Networks, 3, 551
Houk N., 1978, University of Michigan Catalogue of Two-Dimensional Spectral Types for the HD Stars. Vol. 2: Declinations -53 to -40 degrees
Houk N., 1982, University of Michigan Catalogue of Two-Dimensional Spectral Types for the HD Stars. Vol. 3: Declinations -40 to -26 degrees
Houk N., 1994, in Corbally C.J., Gray R.O., Garrison R.F., eds, ASP Conf. Ser. 60, The MK Process at 50 Years. ASP, San Francisco, p. 285

Houk N., Cowley A.P., 1975, University of Michigan Catalogue of Two-Dimensional Spectral Types for the HD Stars. Vol. 1: Declinations −90 to −53 degrees

Houk N., Smith-Moore M., 1988, University of Michigan Catalogue of Two-Dimensional Spectral Types for the HD Stars. Vol. 4: Declinations −26 to −12 degrees

Keenan P.C., McNeil R.C., 1976, An Atlas of Spectra of the Cooler Stars: Types G, K, M, S and C. The Ohio State Univ Press, 1976.

Kent S.M., 1994, Ap&SS, 217, 27

Kurtz M.J., 1982, PhD thesis, Dartmouth College

Lahav O., Naim A., Sodré L., Jr., Storrie-Lombardi M.C., 1996, MNRAS, 283, 207

LaSala, J., 1994, in Corbally C.J., Gray R.O., Garrison R.F., eds, ASP Conf. Ser. 60, The MK Process at 50 Years. Astronomical Society of the Pacific, San Francisco, p. 312

Lindegren L., Perryman M.A.C., 1996, A&ASS, 116, 579

MacKay D.J.C., 1995, Network: Computation in Neural Systems, 6, 469

Morgan W.W., Abt H.A., Tapscott J.W., 1978, Revised MK Spectral Atlas for Stars Earlier than the Sun. Yerkes Observatory, University of Chicago and Kitt Peak National Observatory

Morgan W.W, Keenan P.C., Kellman E., 1943, An Atlas of Stellar Spectra with an Outline of Spectral Classification. University of Chicago Press, Chicago

Morgan W.W., Sharpless S., Osterbrock D., 1952, AJ, 57, 3

Morgan W.W., Whitford A.E., Code A.D., 1953, ApJ, 118, 318

Murtagh F., Heck A., 1987, Multivariate Data Analysis. D. Reidel, Dordrecht

Richard M.D., Lippmann R.P., 1991, Neural Computation, 3, 461

Rumelhart D.E., Hinton G.E., Williams R.J., 1986a, in Rumelhart D.E., McClelland J.L, the PDP Research Group, eds, Parallel Distributed Processing: Explorations in the Microstructure of Cognition, MIT Press, Boston, p. 318

Storrie-Lombardi M.C., Irwin M.J., von Hippel T., Storrie-Lombardi L.J., 1994, Vistas in Astronomy, 38, 331

Vieira E.F., Pons J.D., 1995, A&AS, 111, 393

von Hippel T., Storrie-Lombardi L., Storrie-Lombardi M.C., Irwin M., 1994, MNRAS, 269, 97 (Paper I)

Weaver W.B., 1994, in Corbally C.J., Gray R.O., Garrison R.F., eds, ASP Conf. Ser. 60, The MK Process at 50 Years. ASP, San Francisco, p. 303

Weaver W.B., Torres-Dodgen A.V., 1995, ApJ, 446, 300

Weaver W.B., Torres-Dodgen A.V., 1997, ApJ, 487, 847

Whitney C.A., 1983, A&A, 51, 443